Photoionization study of CH_3SCH_2Cl formed in the reaction system $Cl/Cl_2/CH_3SCH_3$

Bing-Ming Cheng[a] and Eh Piew Chew
Synchrotron Radiation Research Center, No. 1, R&D Road VI, Hsinchu Science-Based Industrial Park, Hsinchu 30077, Taiwan, Republic of China

Jen-Shiang K. Yu and Chin-hui Yu
Department of Chemistry, National Tsing Hua University, 101, Sec. 2, Kuang Fu Road, Hsinchu 30043, Taiwan, Republic of China

(Received 19 July 2000; accepted 22 December 2000)

A photoionization-efficiency spectrum of CH_3SCH_2Cl was measured over the wavelength range 108–142 nm by means of a photoionization mass spectrometer coupled to a synchrotron as the source of radiation. Gaseous CH_3SCH_2Cl was generated in a discharge-flow reactor involving Cl, Cl_2, and CH_3SCH_3 at room temperature *via* these sequential reactions: $Cl+CH_3SCH_3 \rightarrow CH_3SCH_2+HCl$; $CH_3SCH_2+Cl_2 \rightarrow CH_3SCH_2Cl+Cl$. According to the PIE spectrum of CH_3SCH_2Cl thus obtained, the ionization energy is (9.077 ± 0.007) eV. Based on GAUSSIAN-2 calculations, the observed ionization of CH_3SCH_2Cl near the threshold region is likely to form from singlet CH_3SCH_2Cl ionizing to doublet $CH_3SCH_2Cl^+$; the calculated ionization energy 9.064 eV agrees with the experimental value. The adiabatic ionization energy of CH_3SCH_2 and appearance energy of $CH_3SCH_2^+$ from CH_3SCH_2Cl were determined to be (6.884 ± 0.008) eV and (10.007 ± 0.016) eV, respectively; the dissociation energy of the CH_3SCH_2–Cl bond is thus derived to be (72.0 ± 0.6) kcal mol^{-1}. © *2001 American Institute of Physics.*
[DOI: 10.1063/1.1349078]

I. INTRODUCTION

The natural sulfur-containing compound most abundantly released into the atmosphere, dimethyl sulfide (DMS), is produced by phytoplankton in the ocean.[1–3] Oxidation of DMS in the atmosphere might play an important role in the global climate system. Its oxidation is initiated by OH radical;[4,5] oxidation products may form aerosols and nuclei for cloud condensation, which can affect the radiative budget of the atmosphere. Therefore, it is important to understand the kinetics and mechanisms of DMS oxidation and to determine its oxidation products and intermediates.

Field measurements indicate that substantial photochemical activity of chlorine species occurs in both the remote marine boundary layer and coastal urban areas.[6–8] In comparison, for reactions of DMS with Cl and OH,

$$CH_3SCH_3+Cl \rightarrow \text{products}, \quad (1)$$

$$CH_3SCH_3+OH \rightarrow \text{products}, \quad (2)$$

the rate coefficients of reactions (1) and (2) at 298 K are 3.3×10^{-10} and 6.5×10^{-12} cm^3 molecules^{-1} s^{-1}, respectively.[9,10] Chlorine atoms oxidize DMS 50 times more rapidly than analogous reactions involving the OH radical. Reaction of DMS with atomic Cl can thus play a significant role in atmospheric chemistry, and its reaction products and intermediates merit attention in atmospheric research.

Spectral information about species containing sulfur and chlorine is lacking. In previous studies we have applied a discharge-flow reactor with a photoionization mass spectrometer (PIMS) coupled to a synchrotron as the source of ionization to measure photoionization-efficiency (PIE) spectra and ionization energies (IE) of HSCl, CH_3SCl, and C_2H_5SCl.[11–13] In the present work on reaction products and intermediates of sulfur compounds with chlorine, we investigated the photoionization spectrum of CH_3SCH_2Cl from the reaction system $Cl/Cl_2/CH_3SCH_3$. To assess the reliability of our experimental results, we employed *ab initio* calculations on CH_3SCH_2Cl and its cation using the GAUSSIAN-2 (G2) method. Predictions obtained from these calculations are compared to the experimental results. From the photoionization experiments the bond dissociation energies of CH_3SCH_2–H and CH_3SCH_2–Cl are also determined.

II. EXPERIMENTS AND THEORETICAL METHODS

A. Experiments

A photoionization mass spectrometer equipped with a discharge-flow reactor used in this work is described in detail elsewhere;[11–15] only matters pertinent to this experiment are explained here. Vacuum ultraviolet radiation for ionization intersects with gaseous effluents within an extraction region of an ion lens system that focuses ions on the entrance aperture of a quadrupole mass spectrometer operated in the ion-counting mode. Ionization photons are dispersed with a 1 m Seya–Namioka monochromator at the 1.5 GeV storage ring at the Synchrotron Radiation Research Center in Taiwan.[16]

[a]Author to whom correspondence should be addressed. Electronic mail: bmcheng@srrc.gov.tw

We used a grating with 600 grooves/mm to deliver an optimal photon flux in a spectral range 105–185 nm. To suppress radiation of second and higher orders from the grating, a LiF window (thickness 2 mm) was placed between the ionizing chamber and the exit port of the monochromator. Slits of width 0.05–0.2 mm are typical in spectral measurements, corresponding to resolutions of 0.1–0.4 nm. Photoionization spectra are normalized for intensity variation of the ionizing source by procedures described previously.

CH_3SCH_2Cl was generated in the reaction system $Cl/Cl_2/CH_3SCH_3$ *via* the sequential reactions:

$$Cl+CH_3SCH_3 \rightarrow CH_3SCH_2+HCl; \tag{3a}$$

$$CH_3SCH_2+Cl_2 \rightarrow CH_3SCH_2Cl+Cl. \tag{4}$$

These reactions were conducted in a Pyrex flow tube (length 30 cm, i.d. 25 mm). To minimize possible surface reactions, a Teflon tube (i.d. 22 mm) was inserted into the flow tube. Cl atoms were produced by flowing a mixture of He gas containing Cl_2 through a sidearm subjected to microwave discharge. To reduce the background signal due to scattered light, we arranged the discharged gas to flow through a right angle that included a Wood's horn. A mixture of CH_3SCH_3 and He was introduced into the flow tube through the movable injector. Gaseous effluents from the flow tube were sampled into an ionization region of a quadrupole mass spectrometer with differential pumping in three stages.

Typical experimental rates (in STP $cm^3 s^{-1}$) of flow were as follows: He=4–14, Cl_2=0.1–0.4, CH_3SCH_3 =0.2–0.5, He to carry Cl_2=1–2, and He to carry CH_3SCH_3=1–2. The pressure near the reaction region was maintained between 0.7 and 1.5 Torr, resulting in flow speeds in a range of 650–3350 $cm\,s^{-1}$ and reaction times in the range of 8–47 ms. All experiments were carried out at ambient temperature (298±3) K. He (Matheson, >99.9995%) and Cl_2 (Matheson, >99.9%) were used directly without further purification. The liquid sample of CH_3SCH_3 (Aldrich, >99%) was outgassed thoroughly at 298 K, and the first fifth of the sample was discarded before the remaining sample was used.

B. Computational methods

The energetics of CH_3SCH_2Cl and its cation $CH_3SCH_2Cl^+$ were computed with the GAUSSIAN-2 method[17] (G2) using the GAUSSIAN 98 program.[18] The equilibrium structures of the neutral molecule and the positive ion were initially optimized at the Hartree–Fock (HF) level with the 6-31G(d) basis set. The zero-point vibrational energy and harmonic frequencies were calculated at the identical level of theory and scaled with a factor 0.8929. Following optimization using the full second-order Møller–Plesset perturbation method (full MP2) with the 6-31G(d) basis set, an improved geometry of each species was obtained. The G2 energy of $CH_3SCH_2Cl^+$ was derived from the single-point energy including QCISD(T)/6-311G(d,p), MP4/6-311G(d,p), MP4/6-311+G(d,p), MP4/6-311+G($2df,p$), and MP2/6-311+G($3df,2p$) using the optimized geometry at the MP2(full)/6-31G(d) level. The vertical ionization energy (VIE) was deduced from the energy difference between the neutral molecule and its cation at the equilibrium geometry of CH_3SCH_2Cl. Possible vibrational excitation of the cation associated with a vertical transition was not treated explicitly. The zero-point energy, which was evaluated together with the harmonic frequencies from HF/6-31G(d) and scaled with 0.8929 for an optimized geometry of the cation with a structure similar to that of the neutral molecule, was thus used as an approximation. All computational work was done on a Compaq Alpha workstation.

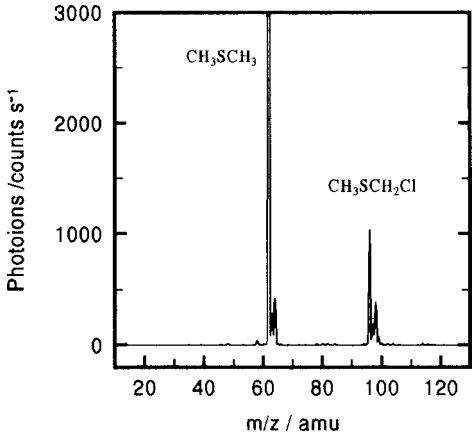

FIG. 1. Mass spectrum in the reaction system $Cl/Cl_2/CH_3SCH_3$ at an excitation wavelength of 124 nm (10.0 eV).

III. RESULTS AND DISCUSSION

A. Formation of products

The target molecule CH_3SCH_2Cl was generated in the reaction system $Cl/Cl_2/CH_3SCH_3$ *via* sequential reactions (3a) and (4). A characteristic mass spectrum obtained under typical flow conditions in this reaction system with the wavelength of ionizing radiation set at 124 nm (10.0 eV) is displayed in Fig. 1. Photoions were detected in significant yield at $m/z=62$ ($CH_3{}^{32}SCH_3^+$), 63 ($^{13}CH_3{}^{32}SCH_3^+$), 64 ($CH_3{}^{34}SCH_3^+$), 96 ($CH_3{}^{32}SCH_2{}^{35}Cl^+$), and 98 ($CH_3{}^{32}SCH_2{}^{37}Cl^+$, $CH_3{}^{34}SCH_2{}^{35}Cl^+$). Except for ions from the reactants, only ions from the CH_3SCH_2Cl product were found to be significant in this system. Reaction (3) might proceed through the following channels:

$$Cl+CH_3SCH_3 \rightarrow CH_3SCH_2+HCl, \tag{3a}$$

$$\rightarrow CH_3SCl+CH_3, \tag{3b}$$

$$\rightarrow CH_3Cl+CH_3S, \tag{3c}$$

$$\rightarrow (CH_3)_2SCl. \tag{3d}$$

Reaction (3) proceeds to form CH_3SCH_2+HCl almost exclusively through channel (a) at 1 Torr and room temperature.[19–21] CH_3SCH_2 radicals were thus produced but subsequently reacted rapidly with Cl_2 to generate CH_3SCH_2Cl. The CH_3SCH_2 radical may react with itself in the reaction system. To avoid this side reaction and to maximize the signal of $CH_3SCH_2Cl^+$, the radical CH_3SCH_2 must react with excess Cl_2 under suitable conditions of flow velocity and position of movable injector through reaction (4).

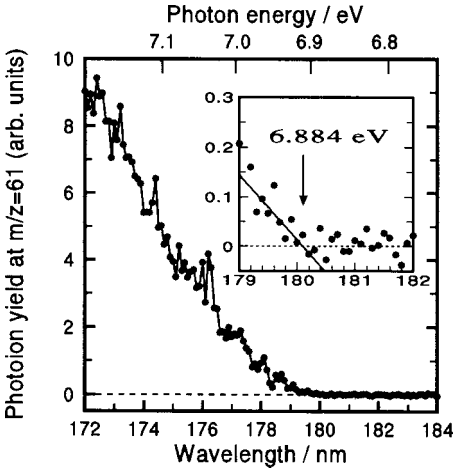

FIG. 2. Photoionization efficiency spectrum of CH_3SCH_2 ($m/z=61$) at a nominal resolution of 0.1 nm and with a step of 0.1 nm. CH_3SCH_2 was produced in the reaction system $Cl/Cl_2/CH_3SCH_3$. An arrow indicates the ionization energy of CH_3SCH_2.

Under such conditions, ions with $m/z=61$ ($CH_3SCH_2^+$) are absent. Ions at $m/z=96$ ($CH_3{}^{32}SCH_2{}^{35}Cl^+$) were typically 3%–15% as intense as the parent ion with $m/z=62$ ($CH_3{}^{32}SCH_3^+$) in this system.

B. IE of CH_3SCH_2

Although ions with $m/z=61(CH_3SCH_2^+)$ are absent under normal conditions of reaction that favors production of CH_3SCH_2Cl, they can be detected under conditions of small Cl_2 concentrations and short reaction times. Even under these conditions, the signal of $CH_3SCH_2^+$ ion is small because the reactivity of the radical is large. Figure 2 displays the ion yield of $m/z=61$ near the threshold region $\lambda=(172-184)$ nm from the reaction system $Cl/Cl_2/CH_3SCH_3$; this spectrum was obtained on monitoring the ion counts at $m/z=61$ that were normalized with respect to relative intensities of the VUV source at varied wavelengths. The spectrum was scanned with steps 0.1 nm at a slit width 0.1 mm, corresponding to a nominal resolution about 0.2 nm. This spectrum has a gradually rising edge, presumably due to small Franck–Condon factors near threshold. Therefore, in this case it was necessary to determine the threshold from the intersection of the baseline with the rising edge fitted to a line. A threshold at (180.1 ± 0.2) nm was obtained, which corresponds to an ionization energy of (6.884 ± 0.008) eV. The listed error includes the uncertainty from a nominal resolution and deviation from the least-squares method that was employed to fit the data points to a straight line. It is important to mention that this determination of $IE(CH_3SCH_2)$ represents an upper limit for the IE because structure was not observed in the photoionization spectrum and a clear, steplike threshold was not obtained.

Stable isomers at $m/z=61$ might exist in four conformers, CH_3CH_2S, *cis*-CH_3CHSH, *trans*-CH_3CHSH, and CH_3SCH_2. In our previous work, the PIE of CH_3CH_2S was measured and its adiabatic IE was determined to be (8.971 ± 0.007) eV.[13] This value is 2.09 eV greater than the IE obtained for $m/z=61$ in this work; thus, CH_3CH_2S is not a candidate for the observed radical. The IE of *cis*-CH_3CHSH, *trans*-CH_3CHSH, and CH_3SCH_2 are calculated to be 6.82, 6.81, and 6.85 eV, respectively.[22] These three theoretical IE are near the experimental value 6.884 eV. Baker and Dyke produced the radical CH_3SCH_2 from a reaction of F with CH_3SCH_3,

$$F+CH_3SCH_3\rightarrow CH_3SCH_2+HF, \tag{5}$$

and determined the IE of CH_3SCH_2 to be (6.85 ± 0.03) eV from photoelectron spectra.[23] This value agrees with the IE obtained in the present study for $m/z=61$, within experimental error. Assuming the same mechanism of hydrogen abstraction occurs in both reactions (5) and (3a), we conclude that the observed photoion at $m/z=61$ is $CH_3SCH_2^+$ that results from direct ionization of the corresponding neutral, CH_3SCH_2.

TABLE I. Predicted ionization energy IE and vertical IE of CH_3SCH_2, CH_3CH_2S, and CH_3SCH_2Cl using the GAUSSIAN-2 method.

Structure	Term	Structure	Term	IE/eV	Vertical IE/eV
CH_3SCH_2	$^2A''$	$CH_3SCH_2^+$	$^1A'$	6.855	7.144
CH_3SCH_2	$^2A''$	$CH_3SCH_2^+$	$^3A'$	9.222	9.893
CH_3CH_2S[a]	$^2A''$	$CH_3CH_2S^+$	$^3A''$	9.077	9.130
CH_3SCH_2Cl	$^1A'$	$CH_3SCH_2Cl^+$	$^2A''$	9.064	9.143
CH_3CH_2SCl[a]	$^1A'$	$CH_3CH_2SCl^+$	$^2A''$	8.978	9.110
CH_3CH_2SCl[a]	$^3A'$	$CH_3CH_2SCl^+$	$^2A''$	6.981	

[a]Reference 13.

In this work, the IE values for doublet CH_3SCH_2 excited to singlet $CH_3SCH_2^+$ and to triplet $CH_3SCH_2^+$ were calculated to be 6.855 eV and 9.222 eV, respectively, as listed in Table I. Accordingly, the photoion at $m/z=61$ observed results from a transition of neutral doublet CH_3SCH_2 to ionic singlet $CH_3SCH_2^+$. The theoretical difference of vertical and adiabatic IE of neutral doublet CH_3SCH_2 to ionic singlet $CH_3SCH_2^+$ is 0.259 eV, see Table I; for comparison, the corresponding difference for neutral doublet CH_3CH_2S and ionic triplet $CH_3CH_2S^+$ is 0.053 eV. The former is almost five times larger than the latter. For CH_3CH_2S the threshold of ionization has an abrupt and distinct step onset, as shown in Fig. 2 of Ref. 13, whereas that of CH_3SCH_2 has a gradually rising edge. These experimental results are consistent with those from theoretical calculations.

C. PIE spectrum and IE of CH_3SCH_2Cl

A PIE spectrum in the spectral range 108–142 nm of the photoion at $m/z=96$ in our reaction system appears in Fig. 3(a). The spectrum was scanned with a 0.2 nm step size and a slit width of 0.1 mm. A background ion-yield spectrum of photoion at $m/z=96$, under the same flow condition except that the microwave discharge to produce the Cl atoms was discontinued, showed only small and regular noise in a featureless structure for wavelengths greater than 108 nm. Hence the PIE spectra displayed in Fig. 3 are those of CH_3SCH_2Cl generated from the reaction and are free of interference. The curve of photoion yield rises abruptly beginning about 137 nm, and ascends continuously to a prominent maximum at 132 nm, then declines gradually until 127 nm.

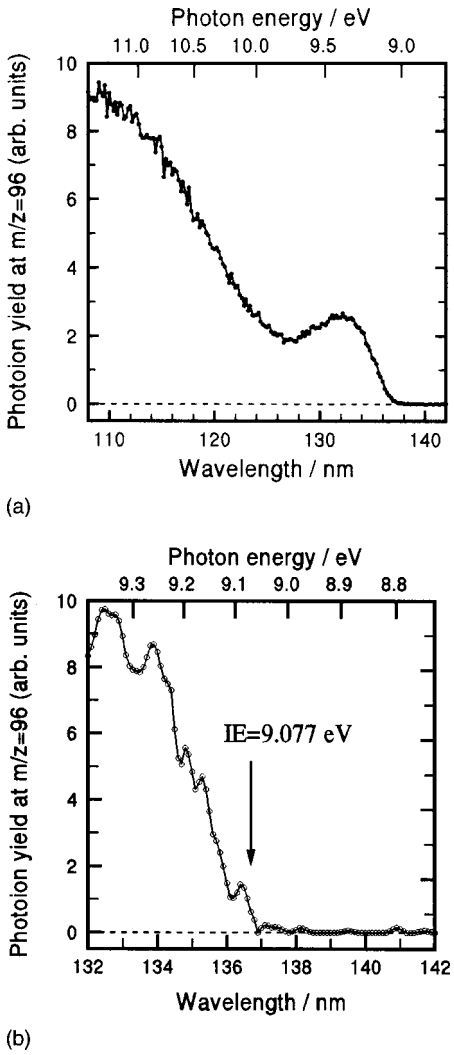

FIG. 3. Photoionization efficiency spectrum of CH_3SCH_2Cl ($m/z=96$) from the reaction system $Cl/Cl_2/CH_3SCH_3$. (a) At a nominal resolution of 0.2 nm and with a step of 0.2 nm over the spectral range 108–142 nm; (b) at a nominal resolution of 0.1 nm and with a step of 0.1 nm in the spectral range 132–142 nm. The arrow indicates the ionization energy of CH_3SCH_2Cl.

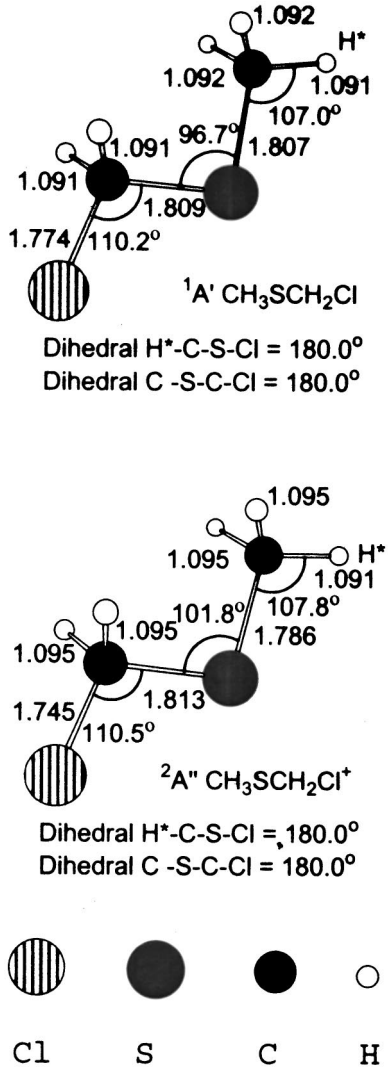

FIG. 4. Geometries of singlet CH_3SCH_2Cl and doublet $CH_3SCH_2Cl^+$ optimized at the MP2(full)/6-31G(d) level. Other important parameters of each species are listed in Table II; the unit of bond length is angstroms.

At this point, the photoion yield curve increases again and possesses no feature to the end of the recorded region.

To improve the determination of the ionization energy of CH_3SCH_2Cl, we performed detailed examination near the threshold region. Figure 3(b) displays the threshold region of CH_3SCH_2Cl in the wavelength range $\lambda=(132-142)$ nm. The spectrum was recorded at a nominal resolution of 0.1 nm with a slit width of 0.05 mm and with a 0.1 nm step size. The PIE spectrum near the threshold features a steplike onset at the long-wavelength end, which is characteristic of direct ionization. The threshold is thus determined by the midrise point, as indicated by the arrow in Fig. 3(b), which is (136.7 ± 0.1) nm. This threshold corresponds to IE$=(9.077\pm0.007)$ eV.

D. Comparison with theoretical calculations

Possible geometries of neutral CH_3SCH_2Cl and its cation were calculated at the MP2(full)/6-31G(d) level, as depicted in Fig. 4. Table II lists predicted energies and some important parameters of these optimized structures, singlet CH_3SCH_2Cl and doublet $CH_3SCH_2Cl^+$. In our previous studies, stable isomers of triplet neutral CH_3SCl and CH_3CH_2SCl were found with such calculations,[12,13] but no

TABLE II. G2 energetics and important structural parameters of CH_3SCH_2Cl and $CH_3SCH_2Cl^+$ optimized at the MP2(full)/6-31G(d) level.

Species	Term	E_{G2}/hartree	S–CH_3 /Å	S–CH_2 /Å	C–Cl /Å	∠S–C–Cl /deg	∠H–C–S /deg	∠C–S–C /deg	Skeletal dihedral /deg
CH_3SCH_2Cl	$^1A'$	−936.517262	1.807	1.809	1.774	110.2	107.0	96.7	180.0(C–S–C–Cl)
$CH_3SCH_2Cl^+$	$^2A''$	−936.184162	1.786	1.813	1.745	110.5	107.8	101.8	180.0(C–S–C–Cl)

TABLE III. Scaled vibrational frequencies in the unit of cm^{-1} of singlet CH_3SCH_2Cl and doublet $CH_3SCH_2Cl^+$ calculated at HF/6-31G(d); a scaling factor 0.8929 is applied throughout.

Vibrational mode	$^1A'$ CH_3SCH_2Cl	$^2A''$ $CH_3SCH_2Cl^+$
1	66.3	45.3
2	174.2	100.4
3	177.9	176.7
4	278.5	277.2
5	694.4	632.7
6	705.3	648.5
7	766.0	778.8
8	870.6	789.3
9	966.7	894.9
10	980.1	995.9
11	1137.1	1128.5
12	1269.5	1268.9
13	1358.7	1351.3
14	1443.6	1398.0
15	1450.9	1406.7
16	1457.0	1410.8
17	2878.5	2880.1
18	2934.9	2918.7
19	2950.4	2969.1
20	2962.6	2986.3
21	2996.1	2999.4

reasonable geometry of neutral triplet CH_3SCH_2Cl was obtained in the present work. This result implies that triplet CH_3SCH_2Cl would not be produced in our reaction system because of its instability.

Structures of both neutral CH_3SCH_2Cl and its cation show C_s symmetry, as shown in Fig. 4. These two species differ mostly in bond lengths C–Cl and S–CH_3, and bond angle ∠C–S–C; the longer are these bonds, the smaller are the bond angles. The bonds C–Cl and S–CH_3 in the neutral species are 0.021 Å and 0.029 Å longer than those in the ion; the bond angle ∠C–S–C of the neutral species is 5.1° smaller than that of the ion. The calculated adiabatic and vertical IE of CH_3SCH_2Cl are 9.064 eV and 9.143 eV, respectively, as listed in Table I. The calculated IE 9.064 eV agrees satisfactorily with the experimental value 9.077 eV. Neutral CH_3SCH_2Cl undergoes a small structural change upon ionization; this condition is reflected in the small difference between adiabatic and vertical IE, $\Delta E = 0.079$ eV (Table I). This is also consistent with the distinct onset at the ionization threshold in the PIE spectrum in Fig. 3.

The PIE spectrum near the threshold region has an underlying vibrational structure; for some spectra we can extract vibrational information about cation and/or neutral species from careful examination. In our work on CH_3SCl, two vibrational frequencies of singlet CH_3SCl and one of doublet CH_3SCl^+ were deduced;[12] for CH_3CH_2SCl, a vibrational frequency of doublet $CH_3CH_2SCl^+$ was derived.[13] Because of rotational broadening and problems of signal-to-noise ratio, the PIE spectrum of CH_3SCH_2Cl near the threshold region yielded no further information for vibrational transition, as shown in Fig. 3(b). Harmonic frequencies calculated for neutral CH_3SCH_2Cl and its cation at HF/6-31G(d) have positive values, indicating that these optimized structures are at local minima. Table III lists these theoretical values scaled by a factor 0.8929 in increasing order.

TABLE IV. Atomic charge densities of CH_3SCH_2Cl, C_2H_5SCl and their cations.

Species	Atomic charge densities					
	H_1[a]	C_1	S	C_2	H_2[b]	Cl
$^1A'$ CH_3SCH_2Cl	0.152	−0.415	−0.054	−0.097	0.175	−0.238
$^2A''$ $CH_3SCH_2Cl^+$	0.217	−0.407	0.506	−0.132	0.232	−0.083
	H_1[a]	C_1	H_2[b]	C_2	S	Cl
$^1A'$ CH_3CH_2SCl[c]	0.149	−0.488	0.143	0.032	−0.194	−0.083
$^2A''$ $CH_3CH_2SCl^+$[c]	0.185	−0.424	0.201	−0.050	0.302	0.215

[a]Average charge of three hydrogen atoms.
[b]Average charge of two hydrogen atoms.
[c]From Ref. 13.

From Mulliken population analysis of HF/6-311 + G($3df$,$2p$) densities, atomic charges of CH_3SCH_2Cl and $CH_3SCH_2Cl^+$ are listed in Table IV, with those of CH_3CH_2SCl and $CH_3CH_2SCl^+$ for comparison.[13] A Mulliken population analysis provides a rough idea about the charge distribution in molecules. For the singlet state of CH_3SCH_2Cl, the carbon atom next to the chlorine atom bears a negative charge, whereas the corresponding carbon atom next to sulfur atom in singlet CH_3CH_2SCl bears a positive charge. Negative charge density concentrates on the sulfur atom of CH_3CH_2SCl, which makes the adjacent chlorine less negatively charged. In contrast, the chlorine atom of CH_3SCH_2Cl bears most of the negative charge, consistent with its more electrophilic property than the next carbon atom. For the doublet state of $CH_3SCH_2Cl^+$, positive charge distributes mostly on the sulfur atom, whereas frontier chlorine atom remains negatively charged because a carbon atom separates S and Cl. The corresponding chlorine atom of doublet $CH_3CH_2SCl^+$ shares positive charge density with its adjacent sulfur atom, so that both sulfur and chlorine atoms become positively charged.

E. Appearance energy (AE) of $CH_3SCH_2^+$

The overall PIE spectrum of $CH_3SCH_2^+$ from the reaction system is displayed in Fig. 5 over the wavelength range 108–184 nm. The spectrum was obtained with a 0.4 nm step size and a slit width of 0.2 mm. As we discussed in Sec. III B, the threshold for ionization of CH_3SCH_2 is at 180.1 nm. The photoion yield curve initially rises at around 180.0 nm in Fig. 5, and it ascends continuously to a maximum at 150 nm, then decreases to about 124 nm. At this point, the photoion yield curve begins to increase again to about 114 nm where the photoion yield curve rises rapidly to 108 nm at which recording ended. The photoion yield spectrum of $CH_3SCH_2^+$ from the reaction system $Cl/Cl_2/CH_3SCH_3$ over the wavelength range 108–184 nm thus features one broad line at 150 nm and two discontinuities at 114 nm and 124 nm.

The photoion yield spectrum of $CH_3SCH_2^+$ from the sample mixture of ~1.5% CH_3SCH_3 in He is shown in Fig. 6; the spectrum was recorded over the wavelength range

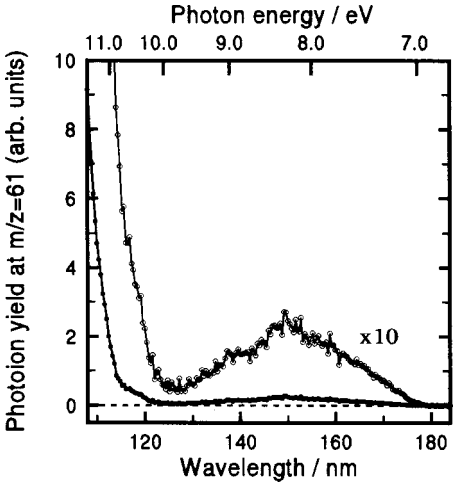

FIG. 5. Photoion yield at $m/z=61$ ($CH_3SCH_2^+$) from the reaction system $Cl/Cl_2/CH_3SCH_3$ over the wavelength range 108–184 nm at a nominal resolution of 0.4 nm and with a step of 0.2 nm. The upper curve is enlarged by 10 times.

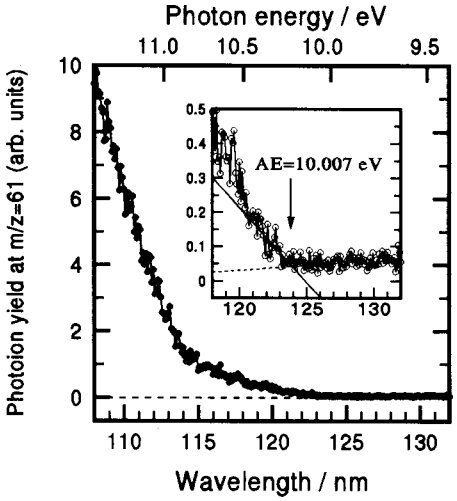

FIG. 7. Photoion yield at $m/z=61$ ($CH_3SCH_2^+$) from the reaction system $Cl/Cl_2/CH_3SCH_3$ over the wavelength range 108–132 nm at a nominal resolution of 0.1 nm and with a step of 0.1 nm. The spectrum in the wavelength range 118–132 nm is shown in detail in the inset. The arrow indicates the appearance energy of $CH_3SCH_2^+$ from CH_3SCH_2Cl.

108–122 nm with 0.1 nm steps and a slit width of 0.1 mm. The observed $CH_3SCH_2^+$ is generated from photofragmentation of CH_3SCH_3 upon ionization,

$$CH_3SCH_3+h\nu\rightarrow CH_3SCH_2^++H+e^-. \tag{6}$$

The appearance energy of $CH_3SCH_2^+$ from CH_3SCH_3 is determined to be (10.866 ± 0.009) eV, (114.1 ± 0.1) nm, as indicated by the arrow in Fig. 6. The appearance wavelength of $CH_3SCH_2^+$ from CH_3SCH_3 is (114.1 ± 0.1)nm, which coincides with a discontinuty in Fig. 5. Thus we conclude that the discontinuity at 114 nm in the photoion yield curve for $CH_3SCH_2^+$ from the reaction system $Cl/Cl_2/CH_3SCH_3$ results from photofragmentation of the parent molecule CH_3SCH_3 upon ionization. Combining the determined value of the adiabatic IE of CH_3SCH_2,

$$CH_3SCH_2+h\nu\rightarrow CH_3SCH_2^++e^-, \tag{7}$$

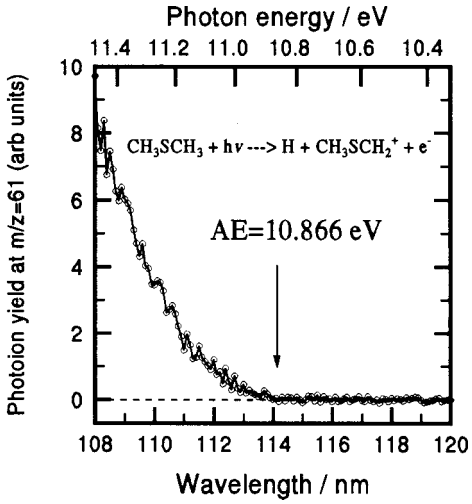

FIG. 6. Photoion yield at $m/z=61$ ($CH_3SCH_2^+$) from 1.5% CH_3SCH_3 in He at a nominal resolution of 0.1 nm and with a step of 0.1 nm. The arrow indicates the appearance energy of $CH_3SCH_2^+$ from CH_3SCH_3.

6.884 ± 0.008 eV, we calculate the bond dissociation energy of CH_3SCH_2–H to be 3.982 eV, corresponding to (91.8 ± 0.2) kcal mol^{-1}. Ng and co-workers measured the distribution of translational energy of H released in laser photodissociation of CH_3SCH_3,

$$CH_3SCH_3+h\nu\rightarrow CH_3SCH_2+H, \tag{8}$$

and obtained the dissociation energy of the CH_3SCH_2–H bond to be (91 ± 2.5) kcal mol^{-1}.[24] For the dissociation energy of the CH_3SCH_2–H bond, our experimental value (91.8 ± 0.2)kcal mol^{-1} agrees satisfactorily with theirs. Considering the observed AE should be corrected for the internal energy of the parent molecule in order to derive the bond energy, the uncertainty in this correction needs to be included and is estimated to be around 0.4 kcal mol^{-1}.[25,26] We thus issued the dissociation energy of the CH_3SCH_2–H bond to be (91.8 ± 0.6) kcal mol^{-1}.

The photoion yield for $CH_3SCH_2^+$ from the reaction system $Cl/Cl_2/CH_3SCH_3$ in the wavelength range 108–132 nm is depicted in detail in Fig. 7; the spectrum was measured with 0.1 nm steps and a slit width of 0.1 mm. The inset shows an expanded section of the spectrum in the wavelength range 118–132 nm; two fitted lines intersect at (123.9 ± 0.2) nm, (10.007 ± 0.016) eV, and define more accurately the other discontinuity in Fig. 5. This discontinuity may result from photofragmentation of reaction product CH_3SCH_2Cl upon ionization,

$$CH_3SCH_2Cl+h\nu\rightarrow Cl+CH_3SCH_2^++e^-. \tag{9}$$

Hence the appearance energy of $CH_3SCH_2^+$ from CH_3SCH_2Cl is (10.007 ± 0.016) eV. With IE=6.884 eV obtained for CH_3SCH_2, we derive a dissociation energy of the C–Cl bond in CH_3SCH_2Cl to be 3.123 eV, which corresponds to (72.0 ± 0.6) kcal mol^{-1} including the uncertainty from the internal energy.

IV. CONCLUSIONS

With a discharge-flow reactor, photoionization mass spectrometer, and synchrotron radiation, we obtained the photoionization spectrum of the product CH_3SCH_2Cl from the system $Cl/Cl_2/CH_3SCH_3$ *via* these sequential reactions: $Cl+CH_3SCH_3 \rightarrow CH_3SCH_2+HCl$; $CH_3SCH_2+Cl_2 \rightarrow CH_3SCH_2Cl+Cl$. The PIE spectrum of CH_3SCH_2Cl rises abruptly beginning about 137 nm, and ascends continuously to a prominent maximum at 132 nm, then declines until 127 nm before increasing again toward 108 nm. An ionization energy (9.077 ± 0.007) eV of CH_3SCH_2Cl is derived from the midrise point of the step onset in the PIE spectrum. According to results from calculations using the G2 method, the observed ionization of CH_3SCH_2Cl near the onset is likely to correspond to formation of ionic doublet $CH_3SCH_2Cl^+$ from neutral singlet CH_3SCH_2Cl upon ionization; our calculated IE 9.064 eV agrees with the experimental value.

The adiabatic IE of CH_3SCH_2 and AE of $CH_3SCH_2^+$ from CH_3SCH_3 were determined to be (6.884 ± 0.008) eV and (10.866 ± 0.009) eV, respectively; the bond dissociation energy of CH_3SCH_2-H is thus derived to be (91.8 ± 0.6) kcal mol^{-1}. This result is consistent with the previous report (91 ± 2.5) kcal mol^{-1} obtained by Ng and co-workers.[24] The AE of $CH_3SCH_2^+$ from CH_3SCH_2Cl was determined to be (10.007 ± 0.016) eV; the bond dissociation energy of CH_3SCH_2-Cl is calculated to be (72.0 ± 0.6) kcal mol^{-1}.

ACKNOWLEDGMENTS

We thank the National Science Council of Taiwan and the Synchrotron Radiation Research Center in Taiwan for support. Calculations were performed on machines at the National Center for High-Performance Computing.

[1] P. A. Spiro, D. J. Jacob, and J. A. Logan, J. Geophys. Res. **97**, 6023 (1992).
[2] T. S. Bates, B. K. Lamb, A. Guenther, J. Dignon, and R. E. Stoiber, J. Atmos. Chem. **14**, 315 (1992).
[3] P. S. Liss, G. Malin, and S. M. Turner, in *Dimethylsulfide: Oceans, Atmosphere, and Climate*, edited by G. Restelli and G. Angeletti (ECSC, EEC, EAEC, Brussels and Luxembourg, 1993), pp. 1–14.
[4] G. S. Tyndall and A. R. Ravishankara, Int. J. Chem. Kinet. **23**, 483 (1991).
[5] D. J. Cooper, J. Atmos. Chem. **25**, 97 (1996).
[6] C. W. Spicer, E. G. Chapman, B. J. Finlayson-Pitts, R. A. Plastridge, J. M. Hubbe, J. D. Fast, and C. M. Berkowitz, Nature (London) **394**, 353 (1998).
[7] A. A. P. Pszenny, W. C. Keene, D. J. Jacob, S. Fan, J. R. Maben, M. P. Zetwo, M. Springer-Young, and J. N. Galloway, Geophys. Res. Lett. **20**, 699 (1993).
[8] H. B. Singh, G. L. Gregory, B. Anderson, E. Browell, G. W. Sachse, D. D. Davis, J. Crawford, J. D. Bradshaw, R. Talbot, D. R. Blake, D. Thornton, R. Newell, and J. Merrill, J. Geophys. Res. **101**, 1907 (1996).
[9] R. Atkinson, D. L. Baulch, R. A. Cox, R. F. Hampson, J. A. Kerr, M. J. Rossi, and J. Troe, J. Phys. Chem. Ref. Data **26**, 521 (1997).
[10] W. B. DeMore, S. P. Sander, D. M. Golden, R. F. Hampson, M. J. Kurylo, C. J. Howard, A. R. Ravishankara, C. E. Kolb, and M. J. Molina, *Chemical Kinetics and Photochemical Data for Use in Stratospheric Modeling*, Evaluation No. 12, JPL Publication 97-4 (Jet Propulsion Laboratory, Pasadena, CA, 1997).
[11] J. Eberhard, W.-C. Chen, C.-h. Yu, Y.-P. Lee, and B.-M. Cheng, J. Chem. Phys. **108**, 6197 (1998).
[12] B.-M. Cheng, E. P. Chew, C.-P. Liu, J.-S. K. Yu, and C.-h. Yu, J. Chem. Phys. **110**, 4757 (1999).
[13] B.-M. Cheng, E. P. Chew, C.-P. Liu, J.-S. K. Yu, and C.-h. Yu, J. Chem. Phys. **111**, 10093 (1999).
[14] B.-M. Cheng and W.-C. Hung, J. Phys. Chem. **100**, 10210 (1996).
[15] W.-C. Hung, M.-Y. Shen, Y.-P. Lee, N.-S. Wang, and B.-M. Cheng, J. Chem. Phys. **105**, 7402 (1996).
[16] P.-C. Tseng, T.-F. Hsieh, Y.-F. Song, K.-D. Lee, S.-C. Chung, C.-L. Chen, H.-F. Lin, T.-E. Dann, L.-R. Huang, C.-C. Chen, J.-M. Chung, K.-L. Tsang, and C.-N. Chang, Rev. Sci. Instrum. **66**, 1815 (1995).
[17] L. A. Curtiss and K. Raghavachari, J. Chem. Phys. **103**, 4192 (1995).
[18] GAUSSIAN 98, Revision A.7, M. J. Frisch, G. W. Trucks, H. B. Schlegel, G. E. Scuseria, M. A. Robb, J. R. Cheeseman, V. G. Zakrzewski, J. A. Montgomery, Jr., R. E. Stratmann, J. C. Burant, S. Dapprich, J. M. Millam, A. D. Daniels, K. N. Kudin, M. C. Strain, O. Farkas, J. Tomasi, V. Barone, M. Cossi, R. Cammi, B. Mennucci, C. Pomelli, C. Adamo, S. Clifford, J. Ochterski, G. A. Petersson, P. Y. Ayala, Q. Cui, K. Morokuma, D. K. Malick, A. D. Rabuck, K. Raghavachari, J. B. Foresman, J. Cioslowski, J. V. Ortiz, A. G. Baboul, B. B. Stefanov, G. Liu, A. Liashenko, P. Piskorz, I. Komaromi, R. Gomperts, R. L. Martin, D. J. Fox, T. Keith, M. A. Al-Laham, C. Y. Peng, A. Nanayakkara, C. Gonzalez, M. Challacombe, P. M. W. Gill, B. Johnson, W. Chen, M. W. Wong, J. L. Andres, C. Gonzalez, M. Head-Gordon, E. S. Replogle, and J. A. Pople, Gaussian, Inc., Pittsburgh, PA, 1998.
[19] R. E. Stickel, J. M. Nicovish, S. Wang, Z. Zhao, and P. H. Wine, J. Phys. Chem. **96**, 9875 (1992).
[20] N. I. Butkovskaya, G. Poulet, and G. LeBras, J. Phys. Chem. **99**, 4536 (1995).
[21] Z. Zhao, R. E. Stickel, and P. H. Wine, Chem. Phys. Lett. **251**, 59 (1996).
[22] Z.-X. Ma, C.-L. Liao, H.-M. Yin, C. Y. Ng, S.-W. Chiu, N. L. Ma, and W.-K. Lee, Chem. Phys. Lett. **213**, 250 (1993).
[23] J. Baker and J. M. Dyke, Chem. Phys. Lett. **213**, 257 (1993).
[24] S. Nourbakhsh, K. Norwood, H.-M. Yin, C.-L. Liao, and C. Y. Ng, J. Chem. Phys. **95**, 5014 (1991).
[25] J. C. Traeger and R. G. McLoughlin, J. Am. Chem. Soc. **103**, 3647 (1981).
[26] T. J. Buckley, R. D. Johnson III, R. E. Huie, Z. Zhang, S. C. Kuo, and R. B. Klemm, J. Phys. Chem. **99**, 4879 (1995).